agriculture

MDPI

Article

Design and Experiment of Precision Seed Metering Device for Flow Adsorption of Quinoa Seeds

Wendong Zhong, Xuan Zhao, Fei Liu *, Hongbin Bai, Wenxue Dong, Hengtong Hu and Xiang Kong

College of Mechanical and Electrical Engineering, Inner Mongolia Agricultural University, Hohhot 01000, China; zwdlrx@emails.imau.edu.cn (W.Z.); zhaoxuan@emails.imau.edu.cn (X.Z.); bhb@emails.imau.edu.cn (H.B.); adong@emails.imau.edu.cn (W.D.); huhengtong@emails.imau.edu.cn (H.H.); 15661453262@163.com (X.K.)
* Correspondence: afei2208@imau.edu.cn

Abstract: This paper proposes a solution to the problem of tight population in the filling area of traditional air suction seed metering devices during quinoa sowing, which leads to inaccurate adsorption. The proposed method disperses the population into a stable seed flow and absorbs the seeds in a flow posture. The flow adsorption precision seed metering device is designed and improved, and the key structure parameters are optimized based on the shape and size parameters of quinoa seeds. A four-factor and three-level response surface orthogonal test is conducted using the Box–Behnken experimental design. The number of seeds, flow angle, negative pressure at the suction hole, and advancing speed are taken as experimental factors, and the qualified index of grain number per hole, qualified index of hole distance, and coefficient of variation of hole distance are used as evaluation indices. The results are optimized using extreme value theory, and it is found that when the seed amount is 5.82 mm, the flow angle is 31.08°, the negative pressure of the air chamber is 1.7 kPa, and the advancing speed is 3.82 km·h^{-1}, and the qualified index of hole number is 94.37%, the qualified index of hole distance is 95.39%, and the coefficient of variation of hole distance is 4.51%. The results are in general agreement with the prediction through the bench validation test, which meets the requirements of quinoa seed metering devices.

Keywords: quinoa; air suction seed-metering device; mechanical–pneumatic coupling; flowing adsorption; small particle size seed

check for updates

Citation: Zhong, W.; Zhao, X.; Liu, F.; Bai, H.; Dong, W.; Hu, H.; Kong, X. Design and Experiment of Precision Seed Metering Device for Flow Adsorption of Quinoa Seeds. *Agriculture* **2024**, *14*, 434. https://doi.org/10.3390/agriculture14030434

Academic Editor: Jacopo Bacenetti

Received: 8 January 2024
Revised: 8 February 2024
Accepted: 28 February 2024
Published: 7 March 2024

1. Introduction

Quinoa is not only rich in protein, vitamins, and minerals but also rich in all of the amino acids necessary for human life activities, which can fully meet the nutritional needs of the human body. It is suitable for the human body as a whole-nutrient food [1,2]. With the growing concern for health issues, quinoa cultivation has been rapidly developed in recent years, and quinoa precision sowing technology as a key link in quinoa cultivation will directly affect the healthy development of the quinoa industry. As the core mechanism of the planter, the seed discharger plays a vital role in seeding quality [3]. Quinoa seeds are small grain size seeds with an average grain size of only 1.5–2 mm, which have a flat shape and low sphericity. Compared with the existing small size seed-metering devices, such as eyelet wheel type [4], hole wheel type [5], scoop type [6], and other mechanical seed dischargers, the quinoa seed shape and size parameters are greatly affected by the quinoa seed size parameters, and the number of seeds taken often fluctuates up and down in the range of 3–15 grains, which is typical of semi-precision sowing. Only realizing hole sowing cannot meet the quinoa precision seeding requirements. Compared with the traditional air suction metering device and mechanical seed-metering device [7,8], there is a certain degree of enhancement, which can control the range of seed extraction in a small range. However, there still exist the problems of suction hole adsorption of multiple seeds, plugging holes, difficulty in clearing the seeds, etc., which impede the further development of precision seeding [9–12].

With the deepening of research, it was found that small-sized seed populations have a high stacking density and are prone to the phenomenon of population siltation. The result leads to a worse population discrete degree and increased interspecific forces in the population. It is difficult to separate single seeds from the population in the planter plate, which results in reseeding and leakage [13]. Therefore, in order to solve the problem of reduced seeding performance due to poor population mobility, different scholars have studied many methods to improve population mobility [14–19]. For example, Li et al. [20,21], Ding et al. [22], Xie et al. [23], etc., installed additional scrambling teeth on the seed discharging disk to agitate the seed population, which increased the degree of population dispersion, reduced the interspecific force, and effectively improved the filling performance of the seed-metering device. Gao et al. [24], Jia et al. [25], Shi et al. [26], and others designed different types of seed-guiding mechanisms, which help to drive the seed towards the suction holes while increasing the mobility of the seed population, thus realizing the orderly and efficient seed filling of the seed discharger. Gaikwad [27], Lu et al. [28], Liu et al. [29,30], and others made the seed population boil by adding an excitation device, thus realizing a directed seed supply or seed dosing. It can be seen that the above scholars only studied the problem of difficult seed filling due to the accumulation of populations from the perspective of how to increase the level of population perturbation. However, they have not solved the problem of difficult seed filling due to the accumulation of populations and interspecific collisions.

In summary, the state of the population in the infilled area has a significant effect on its infilling effect. Therefore, changing the seed supply status of populations in the seed filling area of the seeder can effectively improve the seed filling performance of the seeder, which in turn will enhance the seed discharge performance of the seeder. In this paper, in response to the above problems, a flow adsorption precision planting apparatus with mechanical–pneumatic coupling action was designed with the aim of changing the state of seed supply to the population. It is characterized by making the traditional seed chamber stacking seed supply into a dynamic flow seed supply. This design takes advantage of the unfavorable qualities that quinoa seeds have, namely small particle size and being highly susceptible to airflow. In the flow process, the seed population has a high degree of dispersion, which facilitates the precise adsorption of seeds by suction holes, thus improving the performance of the seed-metering device.

2. Materials and Methods

2.1. Structure and Working Principle of Planting Apparatus

The flow adsorption precision planting apparatus is mainly composed of a seed chamber, seed chamber baffle, seed scooping disk, flange, seed discharging disk, negative pressure air chamber, and so on, and its structure is shown in Figure 1. The core components of the seed discharger are the seed scooping disk, seed discharging disk, and seed chamber baffle. The seed scooping scoops on the seed scooping disk correspond to the adsorption holes of the seed discharge disk and are evenly arranged around the circumference, with a total of 18 scoops. The seed chamber baffle assists the scooping spoon to complete the scooping process on one side, and the other side is provided with a seed flow device to drive the seed along the inclined surface.

The seeding process of the metering device is divided into 4 stages: scooping, flowing, sucking, and casting. When working, the planter plate is driven to rotate counterclockwise by the seeding shaft, and the seed scooping disk is connected to the planter plate through the flange and rotates at the same speed as the planter plate. First, the seed scooping disk rotates from the bottom of the seed chamber to scoop the seeds, and the seed scooping spoon scoops the seeds from the seed chamber with the assistance of the seed chamber stopper. When reaching the seed flow area, the seed scoop is not assisted by the seed chamber baffle. Due to the gravity of the seed population itself, the seeds quickly detach from the scoop and fall into the seed flow device along the seed clearing ramp of the scoop. Then, the seeds are close to the seed discharge disk under the action of the seed flow mechanism and flow along the inclined surface. When the suction hole of A passes through the sloping surface of the seed flow mechanism, it is accurately sucked up from the population of seeds flowing in an orderly manner along the sloping surface. Finally, unaspirated seeds flow back into the seed chamber. At this time, the seeds accurately adsorbed by the suction holes rotate with the planter plate. When it reaches the seed-casting mouth, the seed has no negative pressure effect. Utilizing its own gravity and the initial velocity provided by A (vertically downward), it quickly detaches from the suction hole adsorption and falls into the seed discharge port. This is the completion of the entire seed discharge process, as shown in Figure 2.

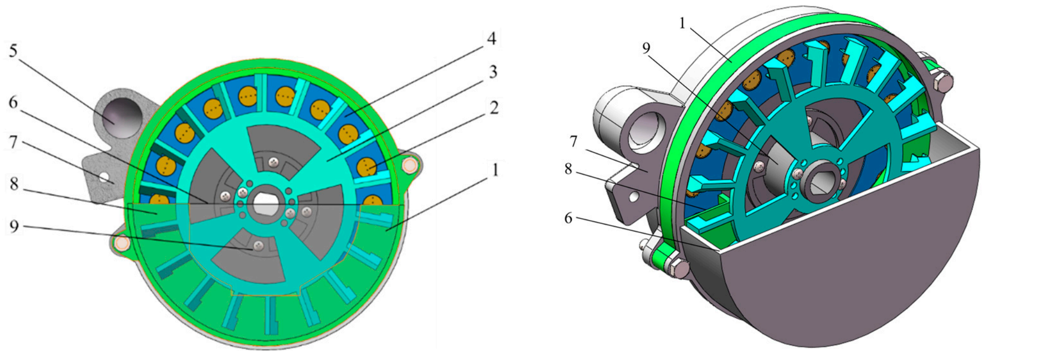

Figure 1. Overall diagram of seed-metering device: 1. seed chamber baffle; 2. adsorption hole; 3. scoop seed plate; 4. planter plate; 5. negative pressure outlet; 6. seed chamber; 7. negative pressure air chamber; 8. rows of seed mouth; 9. flange.

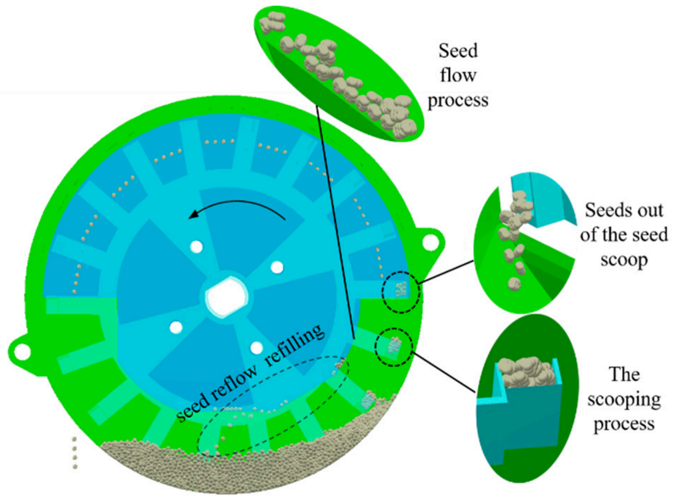

Figure 2. Schematic diagram of the working principle of the seeding apparatus.

2.2. Design of Key Components

2.2.1. Design of the Seed Chamber Baffle

The seed chamber baffle is the core component for forming the flow seed adsorption. The seed chamber baffle mainly consists of a seed flow device, return port, slip seed port, seed discharge port, and positioning hole as shown in Figure 3. On the one hand, the seed chamber baffle assists the scooping spoon in completing the scooping and pouring process, and on the other hand, the seed flow device in the seed chamber baffle makes the seed population form a flow phenomenon. The structural parameters of the flow device determine the flow state of the seed population in the seed filling area, which directly affects the seed filling and adsorption performance of the seed discharger.

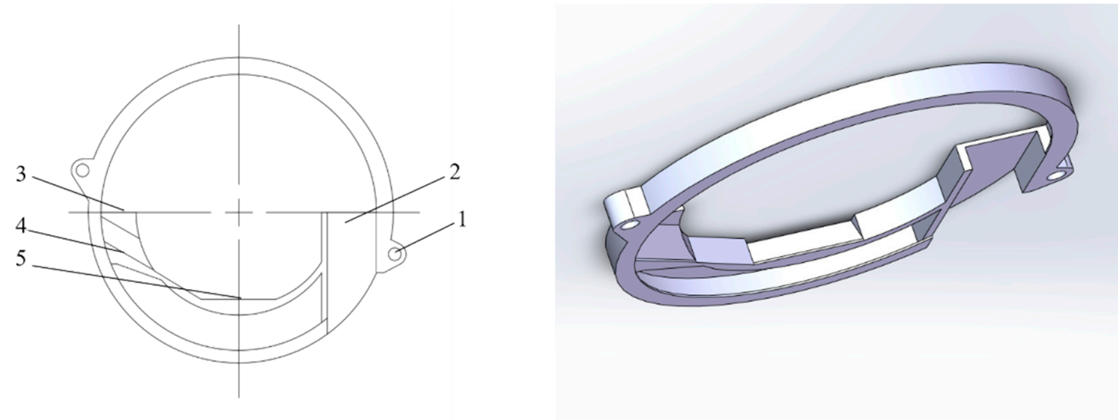

(**a**) (**b**)

Figure 3. (**a**) The schematic diagram of seed chamber baffle: 1. positioning hole; 2. rows of seed mouth; 3. sliding seed mouth; 4. flow seed mechanism; 5. backflow slope; (**b**) three-dimensional model of seed chamber baffle.

The flow seed device is the main structure of the formation of flow adsorption, with flow channel length L, width s_1, cross-section height h, width w, and inverted seed mouth thickness e. The angle θ_2 between the flow seed device and the horizontal line is called the flow angle, θ_1 is called the angle of the repellent seed, and the structure schematic diagram is shown in Figure 4. The size of the flow angle θ_2 is a decisive factor for the state of seed flow of the population in the seed filling area. If the angle is too large, it leads to a faster flow rate of the population in the inclined plane. It results in leakage due to easy breakage of flow and difficulty in the adsorption of seeds. If the angle is too small, the population flow speed in the ramp is too small. It will cause congestion of seed flow, thus losing the significance of seed flow. The purpose of the seed driving angle θ_1 is to drive the seed population close to the seed discharging disk and guide it to flow down along the inclined surface. If the angle is too large, the population cannot flow because the flow channel is too narrow. If the angle is too small, it leads to leakage of suction due to the population being far away from the suction hole of the seed tray. In order to prevent the seed from falling on the thickness of the inverted seed opening, $\mathrm{e} \leq \frac{c}{2}$. In order to make the seed in the flow of seed institutions easily flow and be adsorbed, runner width s1 should be greater than the average thickness of seed c but less than the average thickness of the seed by 1.5 times.

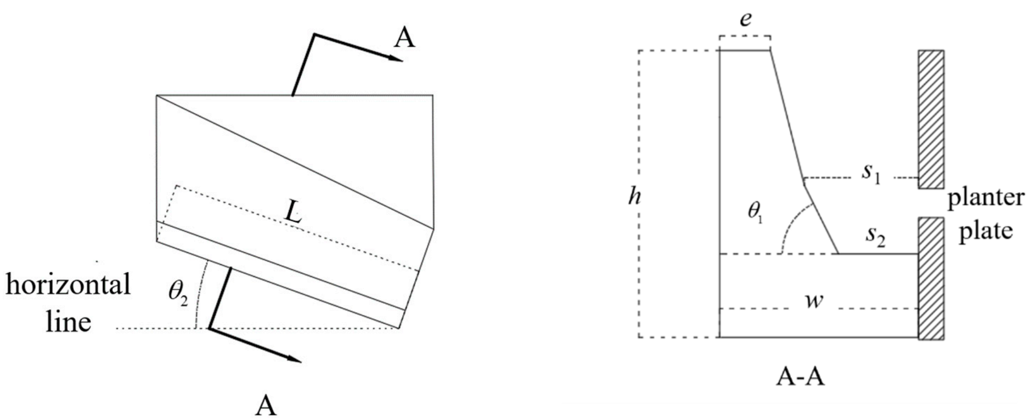

(**a**) (**b**)

Figure 4. Flowing mechanism diagram: (**a**) front view of the seed flow device; (**b**) cutaway view of the seed flow device.

Therefore, it is important to ensure that the seed flow is stabilized. According to the average size of quinoa seeds along three axes, the flow seed structure parameters need to meet the requirements of Equation (1):

$$\begin{cases} s_2 \leq c \\ c \leq s_1 < 1.5c \\ 2e \leq b \\ s_1 = \frac{b}{2\tan\theta_1} + s_2 \end{cases} \tag{1}$$

where the average triaxial dimensions of quinoa were length a = 2.372 mm, width b = 2.201 mm, and thickness c = 1.268 mm.

In this paper, we focus on investigating the effect of flow angle θ_2 on the performance of seed discharge, so it is sufficient to take s_1 = e = 1 mm, θ_1 = 55°, and the flow channel L to transport the seeds to the suction holes passing through.

2.2.2. Design of the Scooping Seed Tray

The seed scooper tray is provided with 18 seed scooping scoops (see Figure 5a). Therefore, the number of seeds scooped by the scoops (seed scooping volume) and the rotational speed of the seed scooping disk directly affect the state of seed flow and the seed filling performance of the seed-metering device. If the amount of seeds scooped is too small, it leads to leakage due to discontinuous seed flow. If the amount of seeds scooped is too much, it leads to the adsorption of multiple seeds in one suction hole due to the increase in the number of seeds on the flow path. In order to avoid collision interference caused by the seeds adsorbed on the suction holes when the population in the scoop is detached from the scoop, the seeds are adsorbed on the suction holes by the seeds. Also, we ensure that when the suction hole passes over the flowing population, the population has formed an orderly flow state (see Figure 5b). Then, it needs to satisfy Equation (2):

$$\frac{D}{2} - R \geq b_1 \tag{2}$$

where D is the diameter (mm) of the seed scooping disk, R is the distance (mm) from the center of the adsorption hole to the center of the shaft, and b_1 is the width (mm) of the seed scooping spoon. Therefore, in this paper, the diameter D of the scooped seed disk is taken as 196 mm.

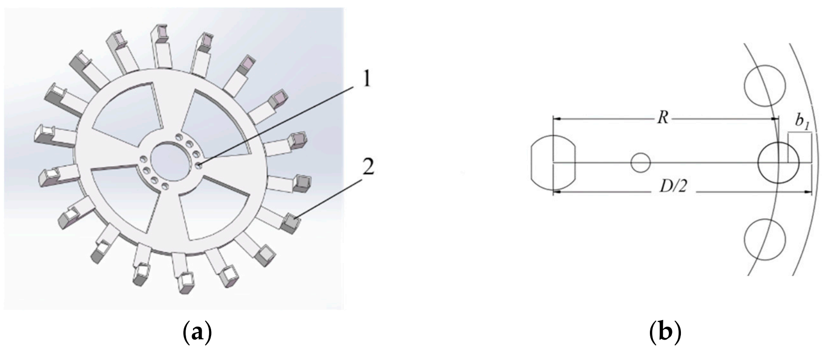

Figure 5. (**a**) Spooning seed plate: 1. positioning hole; 2. take a spoon; (**b**) schematic diagram of the position of the seed scoop and adsorption holes.

The width (mm) of the scooping spoon is b_1, the length (mm) is a_1, and the height (mm) is h_1. The angle between the bottom surface of the scoop and the seed-cleaning ramp is the seed-cleaning angle θ (°), as shown in Figure 6. Then, the volume of the scooping spoon is defined as follows:

$$V = \frac{1}{2} a_1 b_1 h_1 \tag{3}$$

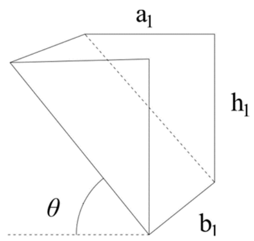

Figure 6. Scoop seed spoon diagram.

2.2.3. Design of Planter Plate

In this paper, the diameter of the disc body of the seed discharge disk is taken as 198 mm, and the relationship between the rotational speed of the seed discharger, the number of holes, and the forward speed is as follows:

$$K = \frac{1000V_{\mathrm{m}}}{60nX_r} \tag{4}$$

where n is the rotational speed (rpm) of the seed discharge disk; V_{m} is the forward speed (km·h^{-1}) of the planter; K is the number of holes in the seed discharge disk; and X_{r} is the theoretical hole distance (mm).

According to the group's previous research, this paper set the disk body on the opening of 18 groups of holes, with two adjacent holes in the middle of the angle of 20°, and the thickness of the disk body is 1.5 mm, as shown in Figure 7. For different types of planting apparatuses, the distribution of holes is also different. At present, the holes have a circular distribution, arc type distribution, and linear distribution. In order to ensure that the adsorbed seeds are quickly moved away from the population and not affected by the flow of seeds, the type of hole has a straight line perpendicular to the radius of the seed discharge disk. In addition, for the small particle size hole seeder, the suction hole spacing has a significant effect on the adsorption performance of the seed discharger, and the interaction force of the two holes spaced 2–5 mm apart has a greater impact. In order to verify the superiority of flow adsorption, the suction hole spacing in this paper is taken as 4 mm. According to the Agricultural Machinery Design Manual, the diameter of the suction hole is generally related to the average width of the seed by the following formula:

$$d_z = (0.64 \sim 0.66)b \tag{5}$$

where d_{z} is the sucking hole diameter, mm, and b is the average seed width, mm. In order to prevent the suction hole from plugging the hole, the sucking hole diameter selected in this paper is 0.8 mm.

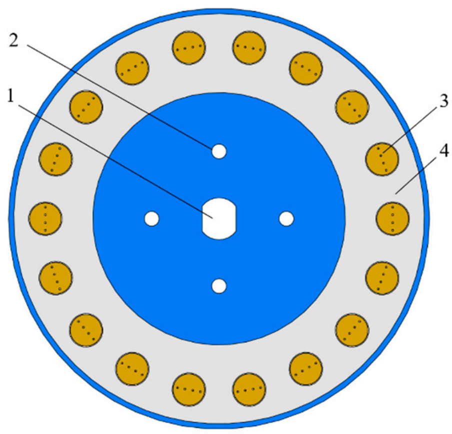

Figure 7. Schematic diagram of seed plate: 1. drive shaft positioning hole; 2. flange positioning hole; 3. adsorption hole; 4. seed plate.

2.3. Flow Process Analysis

Seeds are scooped up by the scoop, the seeds fall out of the scoop and slide down along the inclined plane, the suction holes of the seed discharge tray adsorb the seeds sliding down the inclined plane when they pass through the inclined plane, and this precise adsorption process is called flow adsorption. When the seed population flows on the inclined plane, the seeds flow regularly, which makes it easy for the suction holes to adsorb precisely. In order to investigate the effect of the flow process of the seed population on the adsorption performance, a single seed was taken as the object of study, assuming that the seed is a rigid body, in the same plane without taking into account the friction, interspecies collision force, and other energy losses in the process of the seed sliding down.

The kinetic energy theorem can be expressed as follows:

$$mgH = \frac{1}{2}mv^2 - \frac{1}{2}mv_0^2 \tag{6}$$

where m is the mass of the seed, kg; v_0 is the initial speed of the seed when it is detached from the scooping spoon, m·s^{-1}; v is the speed of the seed when it reaches the position of the suction hole, m·s^{-1}; H is the perpendicular distance from the position of the seed when it is detached from the scooping spoon to the position of the suction hole, m; and g is the acceleration of gravity, which is taken as 9.8 m·s^{-2}.

The following equation is presented:

$$\begin{cases} v_0 = \omega \frac{D}{2} \\ H = r \sin\theta_3 \end{cases} \tag{7}$$

where θ_3 is the seed suction angle, °; ω is the angular velocity of the seed discharge disk, rad·s^{-1}; and r is the distance between the center of the suction hole and the center of the seed discharge disk, m.

The substitution of Equation (9) into Equation (8) yields the following:

$$v = \sqrt{2gr\sin\theta_3 + \frac{1}{4}D^2\omega^2} \tag{8}$$

From Equation (8), it can be seen that speed v is related to diameter D of the seed scooping disk, the radius of rotation r of the center of the suction hole of the seed scooping disk from the center of the axis, the angular velocity ω of the seed scooping disk, and the suction angle θ_3, where seed suction angle θ_3 and flow angle θ_2 are proportional.

2.4. Seeding Performance Test of Seed-Metering Device

2.4.1. Test Equipment and Materials

In order to investigate the influence of seed flow characteristics on the seed discharge performance of the seed discharger, the raw material Meng quinoa 1 quinoa seed from Wu Chuan County, Inner Mongolia, was selected as the experimental research object, and the experimental equipment was the JPS-12 computer vision seed discharger test bench, with the main structure shown in Figure 8.

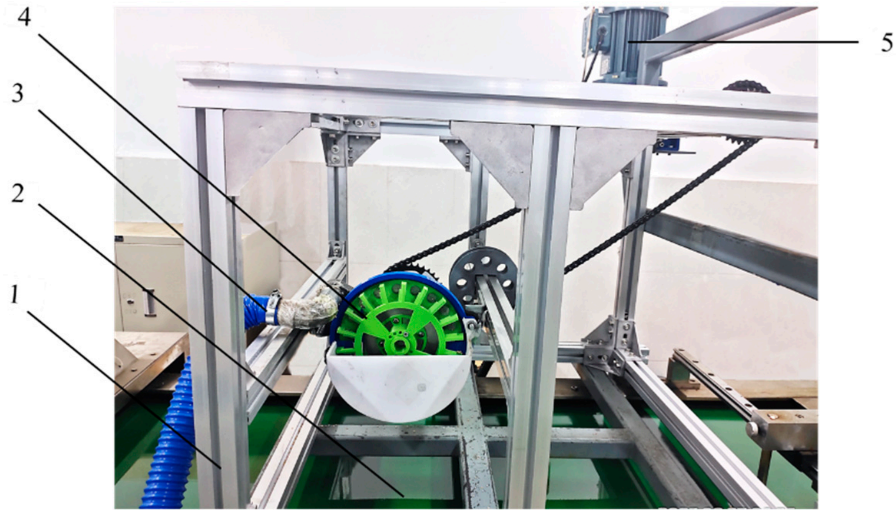

Figure 8. Seeding performance test bench: 1. bench; 2. seeding bed belt; 3. negative pressure trachea; 4. seed-metering device; 5. motor.

2.4.2. Experimental Performance Evaluation Indicators

According to NY/T3687-2020 Technical Regulations for Quinoa Cultivation the theoretical hole spacing is set at X_r = 250 mm, hole spacing X_r is qualified at 235~265 mm, and the number of grains per hole is qualified at 3–5 grains. In this experiment, the qualified index of grain number per hole (Y_1), qualified index of hole distance (Y_2), and coefficient of variation of hole distance (Y_3) were taken as the evaluation indexes of the experiment. Each group of tests was repeated three times, the test results were taken as the average of three times, and 250 hole spacings were taken in each group of tests for statistics.

2.4.3. Single-Factor Experiments

Consider forward speed A, negative pressure B (negative pressure at suction hole), scooped seed volume C, and flow angle D as test factors. The qualified index of grain number per hole (Y_1), qualified index of hole distance (Y_2), and coefficient of variation of hole distance (Y_3) were used as evaluation indexes of the test. A one-factor test was conducted.

2.4.4. Box–Behnken Central Composite Experiment

It was found that forward speed A, negative pressure B, seed scooping volume C, and flow angle D were the key factors affecting the seed discharging performance of the seed discharger, and the response surface design was used to analyze the effects of each factor and its interaction term on the seed discharging performance indexes. The Box–Behnken experimental design principle was adopted to deeply analyze the influence of each factor and its interaction term on the seed discharge performance index. The optimal combination of operating parameters was derived. The coding table of the test factors is shown in Table 1.

Table 1. Coding of test factors.

Level	Factors			
	Forward Speed A/(km·h^{-1})	**Negative Pressure** B/(kPa)	**The Amount of Seed** C/(mm)	**Flow Angles** D/(°)
−1	3.5	1.5	5.5	25
0	4	1.8	6	30
1	4.5	2.1	6.5	35

3. Results and Analysis

3.1. Single-Factor Experimental Results and Analysis

3.1.1. Single-Factor Experiment of the Forward Speed

The forward speed was 3, 3.5, 4, 4.5, and 5 km·h^{-1}; the one-factor test was conducted under the conditions of scooping seed volume of 6.5 mm, negative pressure of 2.1 kPa, and flow angle of 30°; and the results of the test are shown in Figure 9a. From Figure 9a, it can be seen that with the increase in the forward speed, the qualified index of grain number per hole (Y_1) and the qualified index of hole distance (Y_2) firstly increased and then decreased, and the qualified index of grain number per hole started to decrease and the qualified index of hole distance (Y_2) started to decrease when the forward speed was 4.5 km·h^{-1}. Because the forward speed increases, the rotational speed of the seed scooping disk also increases accordingly, and the flow angle is certain, so the amount of seed flow on the seed flow device increases, the dispersion of the population becomes low, and the phenomenon of multiple suction occurs, which leads to a decrease in the qualified index of grain number per hole (Y_1). At the same time, the rotational speed rises and the linear velocity of the adsorbed seeds rises, resulting in a decrease in the qualified index of hole distance (Y_2).

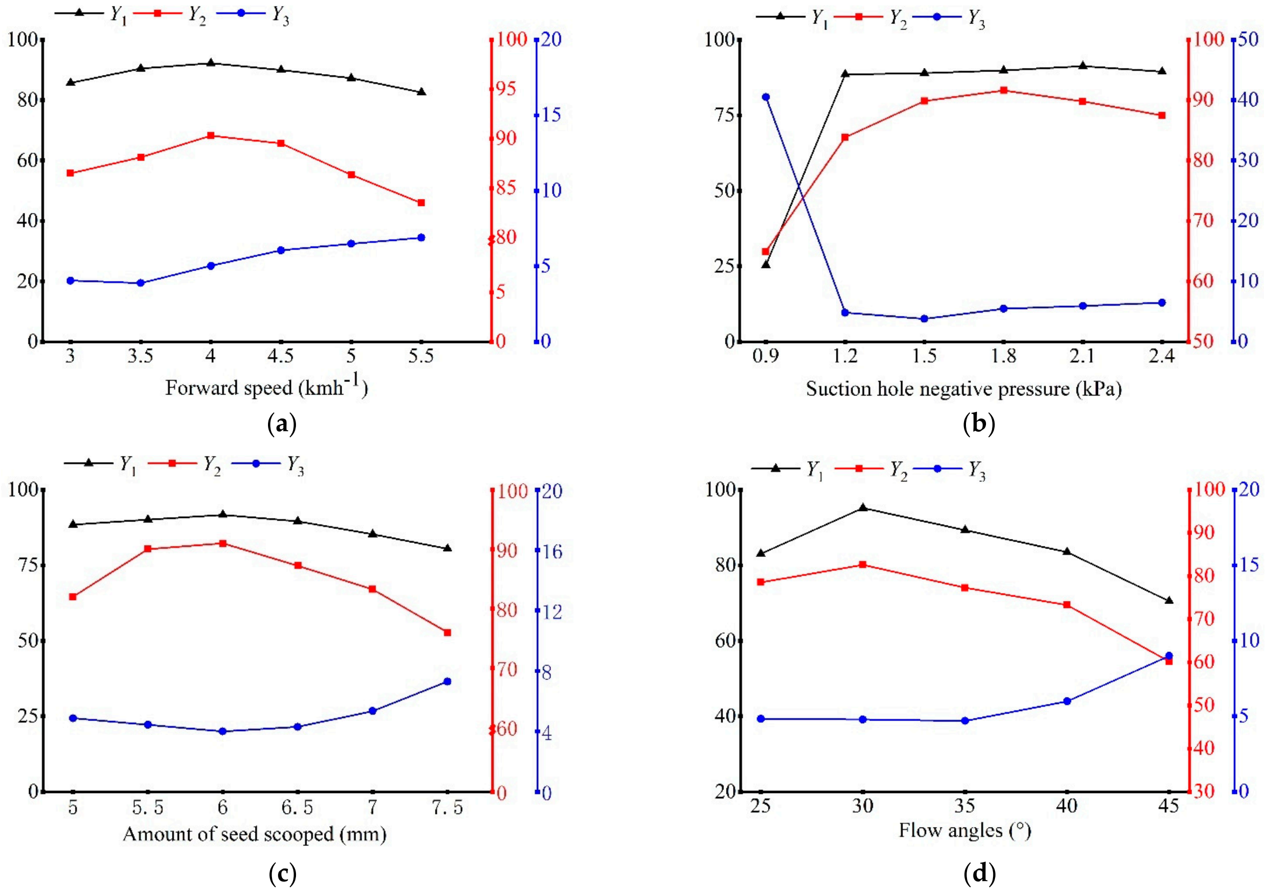

Figure 9. Single-factor test results: (**a**) effect of forward speed on seeding performance; (**b**) effect of suction hole negative pressure on seeding performance; (**c**) effect of spooning amount on seeding performance; (**d**) effect of flow angle on seeding performance.

3.1.2. Single-Factor Experiment of Negative Pressure

Under the conditions of negative pressure of 0.9, 1.2, 1.5, 1.8, 2.1, and 2.4 kPa; forward speed of 4 km·h^{-1}; seed scooping volume of 6.5 mm; and flow angle of 30°, the results of the one-factor test are shown in Figure 9b. From Figure 9b, it can be seen that with the increase in negative pressure, the qualified index of grain number per hole (Y_1) first increased and then leveled off, which can be seen on the flow of the seed device with the right amount of seeds, and the adsorption performance of the seed discharger was not affected by the negative pressure. The qualified index of hole distance (Y_2) first increased and then decreased gently, and the coefficient of variation of hole distance (Y_3) decreased and then tended to stabilize. Because with the increase in negative pressure, the adsorption force of the suction hole increases, and when it reaches the seed discharge port, the seed cannot be dropped in time, resulting in a decrease in the qualified index of hole distance (Y_2).

3.1.3. Single-Factor Experiment of the Amount of Seeds

The results are shown in Figure 9c, from which it can be seen that with the increase in the scooped seed volume, the qualified index of grain number per hole (Y_1) increased and then decreased, the qualified index of hole distance (Y_2) increased and then decreased, and the coefficient of variation of hole distance (Y_3) decreased and then increased. When the amount of seed scooping was 6.5 mm, the amount of seed flow on the seed flow device increased, resulting in a decrease in the flow rate of the seed population, the dispersion became worse, and the phenomenon of multiple suction in one hole occurred. And the adsorption of seeds with multiple suction was unstable, leading to a decrease in the qualified index of hole distance (Y_2) and an increase in the coefficient of variation of hole distance (Y_3).

3.1.4. Single-Factor Experiment of the Flow Angles

Under the conditions of a flow angle of 25°, 30°, 35°, 40°, and 45°; forward speed of 4 km·h^{-1}; scooping volume of 5.5 mm; and negative pressure of 1.8 kpa, a one-way test was conducted, and the results are shown in Figure 9d. From Figure 9d, it can be seen that with the increase in the flow angle, the qualified index of grain number per hole (Y_1) first increased and then decreased, the qualified index of hole distance (Y_2) first increased and then decreased, and the coefficient of variation of hole distance (Y_3) spacing gradually increased. When the flow angle was 35°, the qualified index of grain number per hole (Y_1) began to decline because the flow of seed speed increased, the flow of seed on the flow of the seed device reduced the flow of seeds, and suction holes passing through had difficulty adsorbing.

3.2. Experimental Results and Analysis of the Box–Behnken Central Composite Design

The test results are shown in Table 2. The regression analysis of the test results was carried out using design expert software to analyze the change rule of each test factor on the test indexes. The regression models of each model are shown in Tables 3–5. The significance tests of the regression models for the qualified index of hole grain number Y_1, qualified index of hole spacing Y_2, and coefficient of variation of hole spacing Y_3 were all highly significant, and the results of the test of the misfit term were all non-significant. The R-squared of the models was all greater than 0.87, indicating that the response values exceeded 87% of the variation.

Table 2. Experiment design and result.

No.	Factors				Index		
	A	*B*	*C*	*D*	Y_1 (%)	Y_2 (%)	Y_3 (%)
1	4.5	1.8	6	35	82.56	85.6	9.53
2	4.5	1.5	6	30	79.97	86.79	6.13
3	3.5	1.8	6	35	88.14	91.3	3.47
4	3.5	1.5	6	30	87.36	93.17	6.35
5	4.5	1.8	6	25	81.16	84.25	7.06
6	4	1.5	6	35	88.33	91.6	3.48
7	4	1.8	5.5	25	90.97	92.03	4.09
8	4	2.1	5.5	30	90.03	87.05	5.11

Table 2. *Cont.*

No.	Factors				Index		
	A	*B*	*C*	*D*	Y_1 (%)	Y_2 (%)	Y_3 (%)
9	3.5	2.1	6	30	85.23	83.14	5.02
10	4	1.5	5.5	30	91.01	90.61	3.15
11	4.5	1.8	5.5	30	84.37	85.2	9.35
12	4	1.8	6	30	93.53	93.87	4.48
13	4	2.1	6	25	85.58	83.38	4.34
14	4	1.8	6	30	94.63	94.67	5.99
15	4	1.8	6	30	94.14	94.25	4.36
16	4	1.5	6	25	86.61	90.44	5.12
17	4	2.1	6.5	30	90.11	83.96	8.46
18	4	1.8	6	30	93.24	93.31	5.31
19	4	1.8	6.5	25	86.88	87.66	5.24
20	4.5	1.8	6.5	30	84.4	88.59	8.89
21	4	1.8	6	30	94.22	95.46	5.49
22	4	1.8	5.5	35	92.36	92.14	5.67
23	3.5	1.8	5.5	30	91.96	92.1	5.39
24	4	1.8	6.5	35	91.43	90.21	5.13
25	4	1.5	6.5	30	87.67	91.08	3.16
26	3.5	1.8	6	25	84.03	92.89	4.97
27	3.5	1.8	6.5	30	86.07	89.56	4.81
28	4	2.1	6	35	90.87	87.36	6.37
29	4.5	2.1	6	30	82.53	82.8	9.41

3.2.1. Regression Model of Hole Grain Count Qualification Index

For the qualified index of the number of burrow grains modeled in Table 3, the effects of *A*, *C*, *D*, *AB*, *AC*, *BC*, *BD*, *CD*, A^2, B^2, C^2, and D^2 were highly significant ($p < 0.01$); the effect of *AD* was significant ($p < 0.05$); and the rest of the non-significant factors ($p > 0.05$) should be eliminated. The quadratic polynomial response surface regression model was obtained as follows:

$$Y_1 = 93.95 - 2.32A + 0.28B - 1.18C + 1.54D + 1.17AB + 0.68AC + 0.86AD + 0.89BD + 0.79CD - 6.82A^2 - 3.38B^2 - 0.64C^2 - 2.93D^2 \quad (9)$$

Table 3. Analysis of variance of qualified index of grain number per hole.

Index	Source	Sum of Squares	df	MS	*F*	*p*
Y_1	Model	487.698	14	34.836	131.245	<0.0001 **
	A	64.403	1	64.403	242.644	<0.0001 **
	B	0.963	1	0.963	3.629	0.0775
	C	16.662	1	16.662	62.774	<0.0001 **
	D	28.398	1	28.398	106.990	<0.0001 **
	AB	5.499	1	5.499	20.718	0.0005 **
	AC	8.762	1	8.762	33.010	<0.0001 **
	AD	1.836	1	1.836	6.917	0.0198 *
	BC	2.924	1	2.924	11.017	0.0051 **
	BD	3.186	1	3.186	12.004	0.0038 **
	CD	2.496	1	2.496	9.405	0.0084 **
	A^2	301.827	1	301.827	1137.154	<0.0001 **
	B^2	74.166	1	74.166	279.426	<0.0001 **
	C^2	2.627	1	2.627	9.898	0.0071 **
	D^2	55.645	1	55.645	209.645	<0.0001 **
	Residual	3.716	14	0.265		
	Lock of Fit	2.464	10	0.246	0.787	0.6558
	Pure Error	1.252	4	0.313		
	Cor Total	491.414	28			

Note: * means significant ($0.01 \leq p < 0.05$); ** means extremely significant ($p < 0.01$).

3.2.2. Regression Model for the Hole Spacing Qualification Index

For the burrow distance qualifying index model, as shown in Table 4, the effects of A, B, A^2, B^2, C^2, and D^2 were highly significant ($p < 0.01$); AB and AC were significant ($p < 0.05$); and the rest of the insignificant factors should be eliminated ($p > 0.05$). The quadratic polynomial response surface regression model was obtained as follows:

$$Y_2 = 94.31 - 2.41A - 3B - 0.67C + 0.63D + 1.51AB + 1.48AC + 0.73AD - 0.89BC + 0.71BD + 0.61CD - 3.69A^2 - 4.19B^2 - 1.84C^2 - 2D^2 \tag{10}$$

Table 4. Analysis of variance of hole distance qualified index.

Index	Source	Sum of Squares	df	MS	F	p
Y_2	Model	390.300	14	27.879	17.090	<0.0001 **
	A	69.745	1	69.745	42.754	<0.0001 **
	B	108.000	1	108.000	66.204	<0.0001 **
	C	5.427	1	5.427	3.327	0.0896
	D	4.763	1	4.763	2.920	0.1096
	AB	9.120	1	9.120	5.591	0.0330 *
	AC	8.791	1	8.791	5.389	0.0359 *
	AD	2.161	1	2.161	1.325	0.2690
	BC	3.168	1	3.168	1.942	0.1852
	BD	1.988	1	1.988	1.219	0.2882
	CD	1.488	1	1.488	0.912	0.3557
	A^2	88.169	1	88.169	54.048	<0.0001 **
	B^2	113.773	1	113.773	69.743	<0.0001 **
	C^2	21.885	1	21.885	13.416	0.0026 **
	D^2	26.026	1	26.026	15.954	0.0013 **
	Residual	22.838	14	1.631		
	Lock of Fit	20.189	10	2.019	3.048	0.1471
	Pure Error	2.649	4	0.662		
	Cor Total	413.139	28			

Note: * means significant ($0.01 \le p < 0.05$); ** means extremely significant ($p < 0.01$).

3.2.3. Burrow Distance Coefficient of Variation Regression Models

For the burrow distance coefficient of variation model, as shown in Table 5, the effects of A and A^2 were highly significant ($p < 0.01$), the effects of B and AB were significant ($p < 0.05$), and the rest were insignificant factors that should be eliminated ($p > 0.05$). The quadratic polynomial response surface regression model was obtained as follows:

$$Y_3 = 5.13 + 1.7A + 0.94B + 0.24C + 0.24D + 1.15AB + 0.03AC + 0.99AD + 0.83BC + 0.92BD - 0.42CD + 1.66A^2 - 0.12B^2 + 0.17C^2 - 0.33D^2 \tag{11}$$

Table 5. Variance analysis of variation coefficient of hole distance.

Index	Source	Sum of Squares	df	MS	F	p
Y_3	Model	84.211	14	6.015	6.897	0.0004 **
	A	34.544	1	34.544	39.606	<0.0001 **
	B	10.679	1	10.679	12.243	0.0035 **
	C	0.715	1	0.715	0.820	0.3804
	D	0.667	1	0.667	0.765	0.3965
	AB	5.313	1	5.313	6.092	0.0271 *
	AC	0.004	1	0.004	0.004	0.9497
	AD	3.940	1	3.940	4.518	0.0518
	BC	2.789	1	2.789	3.198	0.0954
	BD	3.367	1	3.367	3.861	0.0696
	CD	0.714	1	0.714	0.819	0.3809
	A^2	17.953	1	17.953	20.584	0.0005 **
	B^2	0.095	1	0.095	0.109	0.7456
	C^2	0.193	1	0.193	0.221	0.6455
	D^2	0.685	1	0.685	0.786	0.3903
	Residual	12.211	14	0.872		
	Lock of Fit	10.294	10	1.029	2.148	0.2400
	Pure Error	1.917	4	0.479		
	Cor Total	96.422	28			

Note: * means significant ($0.01 \le p < 0.05$); ** means extremely significant ($p < 0.01$).

3.3. Impact of Factors on Evaluation Indicators

Using Origin software to process the quadratic polynomial response surface regression model, the effects of different factor interactions on the evaluation indicators can be obtained. According to the response surface, one can fix the level of two of the factors and analyze the effect of the remaining two interactions on each evaluation index. The significance of the effect of the same interaction term on different evaluation indicators is different, and this paper only analyzes the effect of the significant interaction term on the evaluation indicators.

3.3.1. Influence of Factors on the Qualifying Index of Number of Grains in the Hole

1. The interaction of forward speed and negative pressure in the air chamber

As can be seen from Figure 10a, when the scooping volume is 6 mm, the flow angle is 30°, and the negative pressure at the suction hole is at a certain level, with the increase in the forward speed, the number of qualified indexes of the number of grains in the holes first increases and then decreases. When the forward speed is certain, with the increase in negative pressure, the qualified index of the number of grains first increases and then decreases.

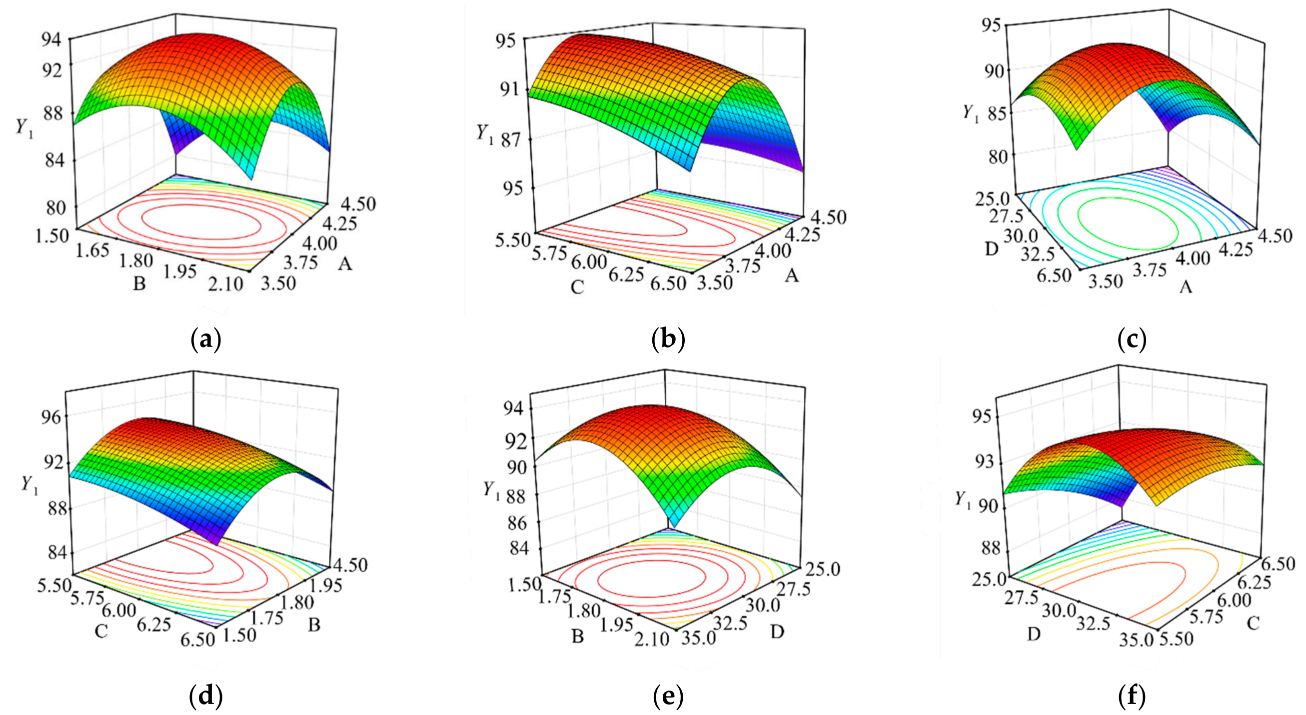

Figure 10. The impacts of interaction factors on the qualified index of grain number per hole. (**a**) AB interaction; (**b**) AC interaction; (**c**) AD interaction; (**d**) BC interaction; (**e**) BD interaction; (**f**) DC interaction.

2. The interaction effect of forward speed and seed scooping volume

From Figure 10b, it can be seen that the negative pressure at the suction hole is 1.8 kPa and the flow angle is 30°, and when the forward speed is at a certain level, with the increase in the scooping volume, Y_1 first increases and then decreases. When the amount of seed scooping is certain, with the increase in forward speed, Y_1 first increases and then decreases.

3. The interaction effect of forward speed and flow angle

From Figure 10c, it can be seen that the negative pressure at the suction hole is 1.8 kPa and the number of scooped seeds is 6 mm, and when the forward speed is at a certain level, with the increase in the flow angle, Y_1 first increases and then decreases. When the flow angle is certain, with the increase in the forward speed, Y_1 first increases and then decreases.

4. The interaction between negative pressure and the amount of seed scooping

From Figure 10d, it can be seen that when the forward speed is 4 km·h^{-1}, the flow angle is 30°, and the negative pressure is at a certain level, Y_1 decreases as the amount of seed scooping increases. At a certain level of seed scooping, with the increase in negative pressure, Y_1 first increases and then decreases.

5. Interaction between negative pressure and flow angle

As can be seen from Figure 10e, when the forward speed is 4 km·h^{-1}, the scooped seed volume is 6 mm, and the negative pressure is at a certain level, with the increase in the flow angle, Y_1 firstly increases and then decreases. When the flow angle is certain, with the increase in the negative pressure, Y_1 first increases and then decreases.

6. Interaction between seed scooping volume and flow angle

From Figure 10f, it can be seen that when the forward speed is 4 km·h^{-1}, the negative pressure is 1.8 kPa, and the seed scooping volume is at a certain level, Y1 increases and then decreases with the increase in the flow angle. When the flow angle is certain, with the increase in the scooped seed volume, Y_1 gradually decreases.

Analysis of the above interaction terms on Y_1 shows that the forward speed, the amount of seed scooping, and the flow angle directly affect the flow of the population and the flow of seed mechanism. When the forward speed or the amount of seed scooping increased, the amount of seed per unit of time into the sliding seed port increased, the amount of seed on the slope increased, the number of collisions of the upper populations of the interspecies increased, and the lower level of mobility of the lower populations was poor, which led to a reduction in the qualification rate; when the flow angle increased, the flow speed increasds, the interspecies collision force increased, the contact time between the suction hole and the seed was shortened, and the difficulty of taking the seed increased, which led to a reduction in the qualification rate; and when the negative pressure increased, the flowing population was affected by the seed on the suction hole, the flow of the population was obstructed, the speed decreased, the number of seeds on the inclined plane increased, and the seed population appeared to have intermittent flow blockage, which led to a reduction in the qualification rate.

3.3.2. Influence of Factors on Qualified Index of Hole Distance

1. Interaction of forward velocity and negative pressure

From Figure 11a, it can be seen that for the scooping amount of 6 mm, flow angle of 30°, and the negative pressure at a certain level, with the increase in forward speed, the rotational speed increases, the initial speed of the seed casting becomes larger due to the seed being lighter, the seed point is not stable, and the hole spacing qualified index is first elevated and then reduced. When the forward speed is certain, with the increase in negative pressure, the suction hole of the seed adsorption increases, resulting in the mouth of the seed casting not being able to immediately detach from the suction hole, and the hole distance qualified index first rises and then decreases; the traditional seed discharger at 1.2 kPa can achieve stable adsorption, and the negative pressure of this test is taken as 1.5~2.1 kPa.

2. Interaction between the amount of seed scooping and forward speed

As can be seen from Figure 11b, the negative pressure is 1.8 kPa and the flow angle is 30°, and when the forward speed is certain, with the increase of the scooping amount of seeds, the amount of seeds on the slant increases; the mobility of the seed population deteriorates; there is the one-hole multi-suck phenomenon, which results in the deterioration of the adsorption stability; and the hole spacing qualification index is firstly elevated and then lowered. When the amount of seed scooping is certain, with the increase in the forward speed, Y_2 first increases and then decreases.

(**a**) (**b**)

Figure 11. The influence of interactive factors on the qualified index of hole distance: (**a**) AB interaction; (**b**) AC interaction.

3.3.3. Influence of Various Factors on the Coefficient of Variation of Hole Distance

As can be seen from Figure 12, when the scooping volume is 6 mm, the flow angle is 30°, and the negative pressure is at a certain level, Y_3 decreases and then increases with the increase in the forward speed. When the forward speed is certain, with the increase in negative pressure, Y_3 gradually increases.

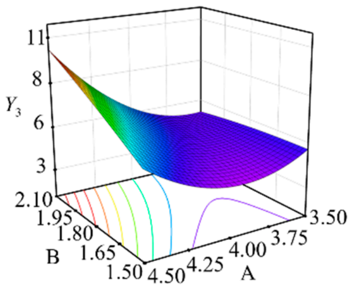

Figure 12. The impacts of interaction factors on the coefficient of variation of hole distance.

3.4. Parameter Optimization and Validation Tests

In order to obtain the optimal combination of the key structural parameters and working parameters of the seed-metering device, the objective function is established with the maximum value of Y_1, the maximum value of Y_2, and the minimum value of Y_3. According to the boundary conditions of each factor, the regression mathematical model is established, and the objective function and constraints are shown in Equation (12). The optimal combination of parameters derived from the solution is a forward speed of 3.82 km·h^{-1}, negative pressure of 1.7 kPa, scooped seed volume of 5.82 mm, flow angle of 31.08°, model-predicted number of holes qualified index of 94.366%, he hole spacing qualified index of 95.387%, and hole spacing coefficient of variation of 4.514%.

$$\begin{cases} \max Y_1 \\ \max Y_2 \\ \min Y_3 \\ s.t. \begin{cases} -1 \leq A \leq 1 \\ -1 \leq B \leq 1 \\ -1 \leq C \leq 1 \\ -1 \leq D \leq 1 \end{cases} \end{cases} \tag{12}$$

The optimization results were subjected to validation tests. Under the same conditions (forward speed of 3.82 km·h^{-1}, negative pressure of 1.7 kPa, scooped seed volume of

5.8 mm, and flow angle of 31°), five replicated tests were conducted. The results show that the average value of the qualified index of grain number per hole (Y_1) is 93.981%, and the five tests can be greater than 92%; the average value of the qualified index of hole distance (Y_2) is 94.267% and can be greater than 93%; and the average value of the coefficient of variation of hole distance (Y_3) is 4.871% and can be less than 5%. The test results and the optimization results comply with the results as shown in Figure 13 and Table 6.

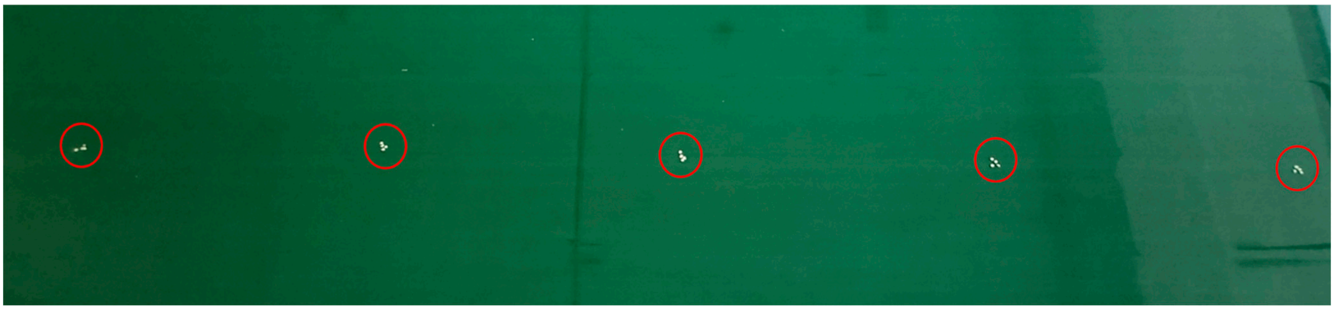

Figure 13. Oil belt seed distribution.

Table 6. Test verification results.

No.	Y_1/%	Y_2/%	Y_3/%
1	93.715	93.859	3.625
2	93.643	92.326	4.168
3	92.714	94.768	5.596
4	95.667	94.705	4.643
5	94.166	95.677	6.323
Mean Value	93.981	94.267	4.871

4. Discussion

The flow adsorption method proposed in this study effectively solves the problem of adsorbing multiple seeds with one suction hole, especially for small particle size seeds. In the traditional small particle size air-absorbent seed discharger, the seed chamber is in direct contact with the seed discharging disk, and the suction holes pass through the seed chamber to adsorb the seeds directly. Although some scholars have improved the adsorption performance by adding a seed stirring device on the surface of the seed discharging disk, there is a probability of contact between the seeds and the suction holes during the working process, which leads to unstable adsorption performance. In this study, firstly, the seed chamber is separated from the seed discharge disk by the seed chamber baffle plate to avoid a large number of seeds coming into direct contact with the suction holes. Then, by scooping the seed plate and the flow seed device, it ensures that the seeds are in contact with the seed discharge tray all of the time and utilizes the relative velocities of the seeds and the suction holes to avoid the problem of multiple seeds adsorbed by a single suction hole. Therefore, the structure and principle of the flow adsorption seed discharger in this study are novel and can provide a reference for small seed precision metering devices. It was found in the experiment that if the number of seeds in the seed filling area was appropriate, the qualified index of grain number per hole first increased and then became flat with the increase in negative pressure in the suction holes. This is consistent with the research results of Liao et al. [14], Li et al. [20], Gao et al. [24], Jia et al. [25], and Shi et al. [26]. This indicates that the flow adsorption seed discharger in this paper can improve the qualified index of grain number per hole.

Although the optimal parameter combination is obtained in this paper and the experimental verification results meet the requirements, there are drawbacks. There is a pulse phenomenon in the seed supply from the scoop, and the amount of seeds scooped per scoop fluctuates greatly, resulting in an unstable seed number and seed population flow on the flow seed device. Subsequent research should change the seed scooping method to continuous seed supply and precisely control the seed quantity to stabilize the seed flow.

5. Conclusions

In this paper, based on the flow adsorption method, a flow adsorption seed discharger was designed, which changes the adsorption mode of the traditional small grain size air-absorbing seed discharger and provides a new idea for the air-absorbing precision seed discharger for small grain size seeds. We conducted a test to verify that the number of hole grains can be controlled in the range of 3–5 grains. The main conclusions are as follows:

1. A quinoa precision seed-metering device based on the flow adsorption method was designed, and its structure and working principle were described. The phenomenon of multiple adsorption in one hole is solved, which leads to a low qualified index of hole grain number because the traditional small particle size seed-metering device has a high population accumulation density in the seed filling area. The population dispersion is improved by the flow seed device, which improves the adsorption performance of the planting apparatus.
2. Through the dynamic analysis of the seed flow process, the influencing factors of the working parameters and structural parameters of the planting apparatus were obtained in the seed flow process and the seed suction process so as to design the seed flow device.
3. The results of the bench verification test show that when the seed scooping volume is 5.82 mm, the flow angle is 31.08°, the negative pressure at suction hole is 1.7 kPa, the forward speed is 3.82 $km \cdot h^{-1}$, the qualified index of grain number per hole (Y_1) is 93.98%, the qualified index of hole distance (Y_2) is 94.27%, and the coefficient of variation of hole distance (Y_3) is 4.87%, which is satisfactory for the quinoa planter to sow quinoa seeds.

Author Contributions: Conceptualization, W.Z. and F.L.; methodology, W.Z., F.L. and X.Z.; software, W.Z., X.Z. and H.B.; validation, W.Z.; formal analysis, W.Z., H.H. and W.D.; investigation, W.Z.; resources, W.Z.; data curation, W.Z. and X.K.; writing—original draft preparation, W.Z.; writing—review and editing, W.Z., F.L., X.Z. and H.B.; supervision, F.L.; funding acquisition, F.L. All authors have read and agreed to the published version of the manuscript.

Funding: This work was supported by The National Natural Science Foundation of China (32060418). The authors give thanks for their generous financial assistance.

Data Availability Statement: The data provided in this study are available upon request from the corresponding author.

Conflicts of Interest: The authors declare no conflicts of interest.

References

1. Rubén, V.; Blanca, H.-L. Nutritional and biological value of quinoa (*Chenopodium quinoa* Willd.). *Curr. Opin. Food Sci.* **2017**, *14*, 1–6.
2. Pereira, E.; Encina-Zelada, C.; Barros, L.; Gonzales-Barron, U.; Cadavez, V.; Ferreira, I.C. Chemical and nutritional characterization of *Chenopodium* quinoa Willd (quinoa) grains: A good alternative to nutritious food. *Food Chem.* **2019**, *280*, 110–114. [CrossRef] [PubMed]
3. Zhao, X.; Zhang, T.; Liu, F.; Li, N.; Li, J. Sunflower Seed Suction Stability Regulation and Seeding Performance Experiments. *Agronomy* **2023**, *13*, 54. [CrossRef]
4. Li, B.H.; Yi, S.J.; Chen, T.; Zhang, X.; Li, Y.F.; Tao, G.X.; Mao, X. Experimental on the Performance of the Combined Type of Seed SowincSeeds with Air Hole and Cell Feed Wheel. *J. Agric. Mech. Res.* **2023**, *45*, 180–185.
5. Yi, S.J.; Chen, T.; Li, Y.F.; Tao, G.X.; Xin, M. Design Test of Millet Hill-drop Seed-metering Device with Combination of Positive-negative Pressure and Hole Wheel. *Trans. Chin. Soc. Agric. Mach.* **2021**, *52*, 83–94, (In Chinese with English Abstract).
6. Zhang, Q.S.; Yu, Q.; Wang, L.; Liao, Y.T.; Wang, D.; Liao, Q.X. Design and Experiment of Scoop-type Precision Hole Metering Device for Rapeseed. *Trans. Chin. Soc. Agric. Mach.* **2020**, *51*, 47–54+64.
7. Liu, R.R. Hole Group Effect Analysis and Performance Test of Quinoa Air-Suction Precision Seed Metering Device. Master's Thesis, Inner Mongolia Agricultural University, Hohhot, China, 2023. [CrossRef]
8. Li, D.P. Discrete Element Analysis and Performance Test of Pneumatic Quinoa Precision Seed Metering Device. Master's Thesis, Inner Mongolia Agricultural University, Hohhot, China, 2021. [CrossRef]

9. Xu, J.; Hou, J.; Wu, W.; Han, C.; Wang, X.; Tang, T.; Sun, S. Key Structure Design and Experiment of Air-Suction Vegetable Seed-Metering Device. *Agronomy* **2022**, *12*, 675. [CrossRef]
10. Li, Z.; Wu, J.; Du, J.; Duan, D.; Zhang, T.; Chen, Y. Experimenting and Optimizing Design Parameters for a Pneumatic Hill-Drop Rapeseed Metering Device. *Agronomy* **2023**, *13*, 141. [CrossRef]
11. Sun, X.; Li, H.; Qi, X.; Nyambura, S.M.; Yin, J.; Ma, Y.; Wang, J. Performance Parameters Optimization of a Three-Row Pneumatic Precision Metering Device for Brassica chinensis. *Agronomy* **2022**, *12*, 1011. [CrossRef]
12. Li, J.H.; Lai, Q.H.; Zhang, H.; Zhang, Z.G.; Zhao, J.W.; Wang, T.T. Suction force on high-sphericity seeds in an air-suction seed-metering device. *Biosyst. Eng.* **2021**, *211*, 125–140. [CrossRef]
13. Han, D.D.; Zhang, D.X.; Jing, H.R.; Yang, L.; Cui, T.; Ding, Y.Q.; Wang, Z.D.; Wang, Y.X.; Zhang, T.L. DEM-CFD coupling simulation and optimization of an inside-filling air-blowing maize precision seed-metering device. *Comput. Electron. Agric.* **2018**, 150. [CrossRef]
14. Liao, Y.T.; Liao, Q.X.; Wang, L.; ZHENG, J.; Gao, P. Investigation on vacuum singulating effect influencing factors of pneumatic precision seed metering device for small particle size of seeds. *Trans. Chin. Soc. Agric. Eng.* **2018**, *34*, 10–17, (In Chinese with English abstract)
15. Ding, L.; Dou, Y.F.; Wang, W.Z.; Xu, Y.F.; He, X.; Qu, Z. Design and Experiment of Seed Metering Device with Combination Hole and Inner Filling for Cyperus esculentus. *Trans. Chin. Soc. Agric. Mach.* **2022**, *53*, 100–115, (In Chinese with English Abstract)
16. Hu, B.; Cai, Y.Q.; Luo, X.; Mao, Z.B.; Li, J.W.; Guo, M.Y.; Wang, J. Theory and experiment of high-speed seed filling in limited gear-shaped side space based on seeds group stress. *J. Jilin Univ.* **2023**, 1–13.
17. Xia, H.M.; Zhou, S.L.; Liu, Y.J.; Zhao, K.D.; Li, Z.W. Design and Test of Directional Vibrating Seed-feeding Device for Flat Solanaceous Vegetable Seeds. *Trans. Chin. Soc. Agric. Mach.* **2022**, *53*, 47–57, (In Chinese with English Abstract)
18. Wang, B.L.; Wang, Z.M.; Luo, X.W.; Zhang, M.H.; Fang, L.Y.; Liu, S.C.; Xu, P. Design and experiment of wedge churning device for pneumatic cylinder-type seed metering device for hybrid rice. *Trans. Chin. Soc. Agric. Eng.* **2019**, *35*, 1–8, (In Chinese with English Abstract)
19. Du, X.; Liu, C.L.; Jiang, M.; Zhang, F.Y.; Yuan, H.; Yang, H.X. Design and experiment of self-disturbance inner-filling cell wheel maize precision seed-metering device. *Trans. Chin. Soc. Agric. Eng.* **2019**, *35*, 2334, (In Chinese with English Abstract)
20. Li, Z.D.; Yang, W.C.; Zhang, T.; Wang, W.W.; Zhang, S.; Chen, L.Q. Design and suction performance test of sucking-seed plate combined with groove-tooth structure on high speed precision metering device of rapeseed. *Trans. Chin. Soc. Agric. Eng.* **2019**, *35*, 12–22. (In Chinese with English abstract)
21. Li, Z.D.; Yang, W.C.; Wu, Y.Y.; He, S.; Wang, W.W.; Chen, L.Q. Performance analysis and experiments of seed filling assisted by groove-tooth of pneumatic disc precision metering device for rapeseed. *Trans. Chin. Soc. Agric. Eng.* **2020**, *36*, 57–66, (In Chinese with English Abstract)
22. Ding, L.; Yang, L.; Liu, S.R.; Yan, B.X.; He, X.T.; Zhang, D.X. Design of air suction high speed precision maize seed metering device with assistant seed filling plate. *Trans. Chin. Soc. Agric. Eng.* **2018**, *34*, 1–11, (In Chinese with English Abstract)
23. Xie, D.B.; Zang, C.L.; Wu, X.Q.; Wang, W.W.; Liu, L.C.; Chen, L.Q. Design and Test of Garlic Seed Placer with Seed Disturbing Tooth Assisted Air Suction. *Trans. Chin. Soc. Agric. Mach.* **2022**, *53*, 47–57, (In Chinese with English Abstract)
24. Gao, L.P.; Shi, B.B.; Liao, Q.X.; Zhang, B.X.; Zheng, J.; Liao, Y.T. Seeding performance of conical-hole seeding plate of the positive and negative pressure combination precision seed metering device for rapeseed. *Trans. Chin. Soc. Agric. Eng.* **2022**, *38*, 22–33, (In Chinese with English Abstract)
25. Jia, H.L.; Chen, Y.L.; Zhao, J.L.; Wang, J.X.; Guo, M.Z.; Zhuang, J. Design and Experiment of Pneumatic-mechanical Combined Precision Metering Device for Soybean. *Trans. Chin. Soc. Agric. Mach.* **2018**, *49*, 75–86+139, (In Chinese with English Abstract)
26. Shi, S.; Zhou, J.L.; Liu, H.; Fang, H.M.; Cun, S.C.; Zhang, R.F. Design and Experiment of Pneumatic Precision Seed-metering Device with Guided Assistant Seed-filling. *Trans. Chin. Soc. Agric. Mach.* **2019**, *50*, 61–70, (In Chinese with English Abstract)
27. Gaikwad, B.B.; Sirohi, N.S. Design of a low-cost pneumatic seeder for nursery plug trays. *Biosyst. Eng.* **2008**, *99*, 322–329. [CrossRef]
28. Lu, F.Y.; Ma, X.; Qi, L.; Xing, X.P.; Li, H.W.; Guo, L.J. Theory and Experiment on Vibrating Small-amount Rice Sowing Device. *Trans. Chin. Soc. Agric. Mach.* **2018**, *49*, 119–128+214, (In Chinese with English Abstract)
29. Liu, C.L.; Wang, C.; Song, J.N.; Du, X.; Zhang, F.Y. Design and Seed-filling Test of Cell-type Precision Seed-metering Device with Vibration Technology. *Trans. Chin. Soc. Agric. Mach.* **2018**, *49*, 108–115, (In Chinese with English Abstract)
30. Liu, C.L.; Wang, Y.L.; Du, X.; Song, J.N.; Wang, J.C.; Zhang, F.Y. Filling performance analysis and verification of cell-belt rice precision seed-metering based on friction and repeated filling principle. *Trans. Chin. Soc. Agric. Eng.* **2019**, *35*, 29–36, (In Chinese with English Abstract). [CrossRef]